Conference on Modelling Fluid Flow (CMFF'22)
The 18th International Conference on Fluid Flow Technologies
Budapest, Hungary, August 30-September 2, 2022

MULTIMODAL HEMODYNAMIC EVALUATION OF VESSEL WALL ENHANCED CEREBRAL DRAINING VEINS FOR THE ASSESSMENT OF ARTERIOVENOUS MALFORMATIONS

Janneck Stahl[1], Sylvia Saalfeld[2], Laura Stone McGuire[3], Denise Brunozzi[3], Ali Alaraj[3], David Hasan[4], Philipp Berg[1]

[1] Corresponding Author. Department of Fluid Dynamics and Technical Flows, Research Campus *STIMULATE*, University of Magdeburg, Universitätsplatz 2, 39106 Magdeburg, Germany. E-mail: janneck.stahl@ovgu.de
[2] Department of Simulation and Graphics, Research Campus *STIMULATE*, University of Magdeburg, Germany. E-mail: sylvia.saalfeld@ovgu.de
[3] Department of Neurosurgery, University of Illinois, Chicago, USA. E-mail: alaraj@uic.edu
[4] Duke Neurological Disorders Clinic, Durham, NC, USA. E-mail: david.hasan@duke.edu

ABSTRACT

Cerebral arteriovenous malformations (AVMs) are a neurovascular disease where the arteries directly connecting to the veins via a nodular nidus. This study investigates the relationship between wall enhancement, referring to a local increase of the intensity in vessel wall magnetic resonance imaging (VW-MRI), and hemodynamics along AVM draining veins. Image-based blood flow simulations using computational fluid dynamics (CFD) were conducted based on 3D models of the venous domain for eight AVM cases. The areas of the vessel wall enhancement were manually extracted from VW-MRI data, co-registered and mapped onto the luminal surface models. Hemodynamic results of draining veins containing enhancement are compared with non-enhanced draining veins of the AVM cases. Global comparison of shear-related draining vein hemodynamics reveals a mean decrease of time-averaged wall shear stress and oscillatory shear index, while the relative residence time demonstrates an increase in draining veins harboring vessel wall enhancement. Furthermore, the enhanced walls are assessed locally in terms of shear-related hemodynamic parameters and related to the non-enhancing area of the corresponding draining veins. In conclusion, this initial multimodal investigation of hemodynamics in AVM draining veins allows for precise prediction of occurring shear-related phenomena, especially in areas of vessel wall enhancement and improves the understanding of this complex neurovascular pathology.

Keywords: arteriovenous malformations, cerebral blood flow, CFD, hemodynamics, wall enhancement

NOMENCLATURE

$AWSS$	$[Pa]$	time-averaged wall shear stress
OSI	$[-]$	oscillatory shear index
RRT	$[1/Pa]$	relative residence time

1. INTRODUCTION

Cerebral arteriovenous malformations (AVMs) contain a complex vasculature. Instead of a capillary bed, a tangle-like nidus occurs locally, directly connecting the arterial and venous vascular system. The challenging neurovascular disease shows a prevalence of 18 per 100,000 and is responsible for 2% of all hemorrhagic strokes [1, 2]. Due to the lack of microcirculation structures between the vascular systems, hemodynamic stressors such as steep pressure gradients and increased flow might alter brain vasculature. Additionally, these undesired physiological conditions might cause a further weakening of the vessel walls resulting in hemorrhage, which can be found in 50% of cerebral AVMs [3].
While most research studies only assess the morphology and hemodynamics of AVM arteries and the nidus, knowledge with respect to the hemodynamics for the venous areas is limited [4, 5, 6]. Already existing studies have simulated blood flow in cerebral veins and investigated various hemodynamic aspects, however, they are not related to existing pathologies such as AVMs [7, 8]. Therefore, this study particularly focusses on the AVM draining veins.
Due to improvements in medical imaging the complex morphologies of AVMs could be diagnosed more precisely. These include vessel wall magnetic resonance imaging (VW-MRI), which can provide indications of histologic changes in the vessel wall by enhanced intensity values in these areas, which

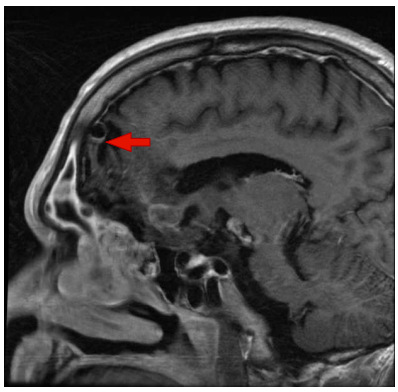

Figure 1. VW-MRI from saggital view of an AVM draining vein. The red arrow indicates signal enhancement in the vessel wall.

is called wall enhancement (see Figure 1). Furthermore, studies have shown that wall enhancement could be assumed as a possible biomarker for vessel wall inflammation [9, 10, 11].
The present study aims to investigate blood flow along the vessel wall of signal-enhanced AVM draining veins by multimodal hemodynamic modeling. Through an interdisciplinary approach, initial observations of various hemodynamic parameter changes in these areas are carried out. The simulation results based on computational fluid dynamics (CFD) will then be correlated with the enhanced local vascular areas.

2. MATERIAL AND METHODS

2.1. Image Data

Eight AVM patients are included in the study. Of the total 15 identified draining veins, seven draining veins (46.7 %) show a local vessel wall signal enhancement in the VW-MRI data. Multimodal medical image data are provided for all patients. First, 3D rotational angiography (3DRA) image data are available, which have a high spatial resolution of the arterial area as well as the nidus. The focus is especially on the draining veins, exiting from the nidus and merging into the deep veins. For this reason, magnetic resonance venography (MRV) data, which particularly resolves the venous vascular area, is used for the morphological studies. In addition to imaging data depicting patient-specific vascular anatomy, intravascular flow measurements based on 2D phase contrast magnetic resonance imaging (2D PC MRI) are available. Flow quantifications perpendicular to the corresponding vessel axis were acquired using non-invasive optimal vessel analysis (NOVA) software (VasSol Inc, River Forest, IL) [12]. These flow rates can be used for realistic boundary conditions of the hemodynamic simulations.

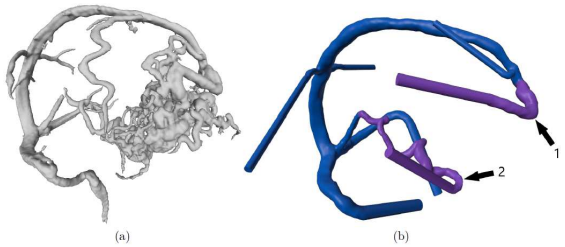

Figure 2. Segmented 3D models of vascular anatomy of an exemplary case: (a) Initial segmentation from the MRV data including nidus. (b) Processed model without nidus with the two draining veins colored in purple and labeled.

2.2. Multimodal Image Segmentation and 3D Model Extraction

The image segmentation and surface mesh generation was carried out using MeVisLab 3.4.1 (MeVis Medical Solutions AG, Bremen, Germany). As the focus of this study is on the venous region and in particular on the draining veins of the AVM, the segmentations of the vascular structures are primarily realized based on the MRV data. By using threshold-based segmentation before converting the segmentation masks into triangulated surface meshes, initial 3D models are provided (see Figure 2).
To perform a successful hemodynamic simulation, the surface mesh should be as free of artefacts as possible. For this reason, manual corrections on the initial segmentations are necessary, which are performed with the 3D modeling software Blender 2.9 (Blender Foundations, Amsterdam, Netherlands). Initially, the nidus are removed using boolean cuts, since this is not the focus of the study, but rather the veins that drain out of it. Fused vessel areas are separated and artifacts appearing on the surface mesh are removed. Since edged vessel areas are created during these post-processing steps local laplaician smoothing is conducted to maintain a realistic vessel shape in these regions. Furthermore, the vascular 3D models are prepared for the subsequent hemodynamic simulations by cutting and extruding the in- and outlet cross-sections perpendicular to the vessel axis (see Fig. 2).

2.3. Segmentation and Co-Registration of the Wall Enhancement

To identify the enhanced areas VW-MRI images from coronal, axial and sagittal planes were marked by an experienced neurosurgeon. Based on the markers, these areas are manually extracted in MeVisLab using the CSO (Contour Segmentation Object) library before converting them into 3D models. In order to visualize the enhanced areas on the vascular surface of the previously segmented venous models, co-registration is required, since VW-MRI and MRV data are not located in the same coordinate system. The registration is performed using a rigid body 3D

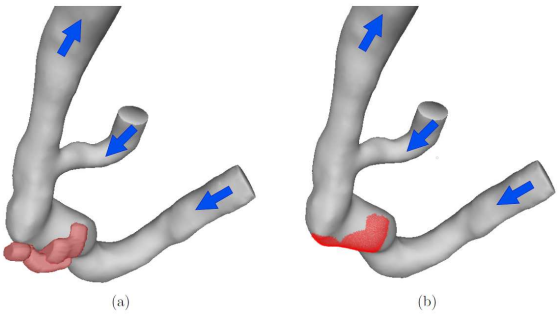

Figure 3. Mapping of the segmented structures of the wall enhancement shown in red (a) to the vessel surface of the draining vein (b). The blue arrows indicate the direction of the blood flow.

image-based registration pre-implemented in MeVisLab. By shifting the VW-MRI data into the space of the MRV data, a corresponding transformation matrix results, which is subsequently applied to the enhancement models. Thus, the wall enhancement extraction moves exactly to the luminal vessel wall. Since the venous models only indicate luminal information, the areas of enhancement are mapped exactly to the venous surface. This results in an area of enhancement lying exactly on the venous vessel wall, where the hemodynamics can be examined locally (see Figure 3).

2.4. Hemodynamic Simulation

Based on the presented segmentation results, hemodynamic simulations are carried out to assess the individual flow situation and enable a precise evaluation at wall enhanced areas, respectively. Here, numerical simulations are acquired with a CFD approach using a finite-volume-based solver.

In a first step, spatial discretization is perfomed using STAR-CCM+ 2020.1 (Siemens Product Lifecycle Management Software Inc., Plato, TX, USA). Specifically, polyhedral as well as prism cells with a base size of 0.25 mm were used for the generation of the underlying volume meshes resulting in a number of elements ranging from 1.5 to 3.7 million depending on the respective vascular domain. The creation of three prism layers with a growth rate of 1.3 is of particular importance to account for the occurring velocity gradients especially due to narrow vessel courses.

To realize the time-dependent blood flow simulations, patient-specific in- and outflow boundary conditions are defined for each model. For all cases, flow quantifications are available for the main in- and outflow vessels as well as for the draining veins by means of 2D PC MRI measurements of the time-dependent volume rate.

At the vessel cross sections, where no flow quantification measurements are available, constant pressure values are assumed based on the literature [13]. Blood is treated as an incompressible ($\rho = 1055\ \frac{\mathrm{kg}}{\mathrm{m}^3}$), Newtonian ($\eta = 4\ \mathrm{mPa} \cdot \mathrm{s}$) fluid and laminar flow

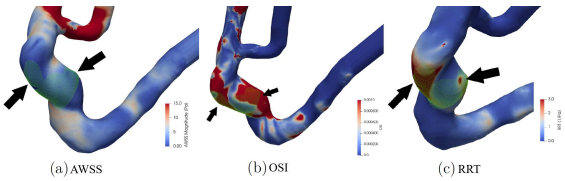

Figure 4. Qualitative representation of AWSS (a), OSI (b), RRT (c) on the vessel surface in the area of draining veins for an exemplary case with overlaid wall enhancement (green, recall Fig. 3) and marked areas showing a local hemodynamic change compared to the surrounding area.

conditions were assumed. Furthermore, the vessel walls follow the rigid wall condition, as no further information is available. For all patient-specific models, two cardiac cycles are simulated. The first cycle represents the initialization of the simulation, while the second provides the periodic solutions. Consequently, only the last cycle is included in the following consideration.

2.5. Analysis

For hemodynamic evaluation, three shear-related parameter are calculated using the 3D post-processing software EnSight 10.2.8 (ANSYS, Inc., Canonsburg, PA, USA).

- Time-averaged Wall Shear Stress (AWSS) describes the tangential shear stress along the luminal vessel wall.
- Oscillatory Shear Index (OSI) is a metric to describe the change in magnitude and direction of wall shear stress throughout one cardiac cycle.
- Relative Residence Time (RRT) provides information about the blood flow distribution at the vessel wall.

3. RESULTS

3.1. Qualitative Results

For the qualitative analysis, the calculated parameters were displayed on the vessel wall of the 3D venous models. Since the signal ehancement extracted from the VW-MRI data is present on the vessel wall as well, visual characteristics of local hemodynamic properties can thus be detected in these areas. For all the draining veins with wall enhancement, initial qualitative tendencies can be observed, as exemplified in Figure 4. In the area of the enhancement, a locally decreased AWSS and locally increased RRT can be recognized. In contrast, the OSI shows no clear hemodynamic tendency in this area.

3.2. Quantitative Results

In addition to the qualitative observations, quantifications are performed along the vessel surface. First, all identified draining veins for the eight patient

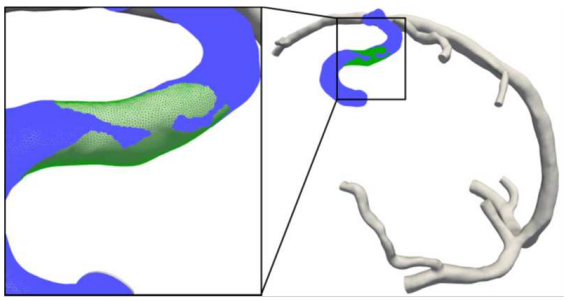

Figure 5. Illustration of enhanced area (green) on the remaining draining vein without enhancement (blue) for an exemplary case.

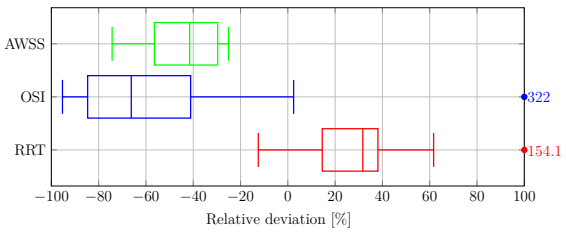

Figure 6. Boxplots of the mean relative deviations of the shear-related parameters within enhanced areas compared to areas of the draining vein without enhancement. The respective outliers for the OSI and RRT, which were removed due to the scaling from -100 % to 100 %, are indicated on the right side of the boxplot.

models are included in the analysis and a global comparison is carried out. The three calculated hemodynamic parameters (AWSS, OSI and RRT) averaged over all seven veins showing wall enhancement were compared with those averaged over all eight veins with no wall enhancement (see Table 1). Global comparison of shear-related hemodynamics of total draining veins thus shows a mean decrease in AWSS (-72.8 %) and OSI (-89.5 %), whereas RRT in draining veins with wall enhancement of the vessel wall shows an increase (+86.9 %).

Table 1. Results of the global hemodynamic comparison

Parameter	Enhanced	Non-enhanced
AWSS [Pa]	1.75	6.42
OSI	$1.43 \cdot 10^{-3}$	$1.36 \cdot 10^{-2}$
RRT [1/Pa]	0.98	0.53

In addition to the global quantification, particular consideration is given to the local hemodynamic characteristics in the area of extracted signal enhancement. For this purpose, the parameters are calculated both directly locally in the enhanced areas and on the areas of the draining veins, which present with no enhancement (see Figure 5). The calculations of the relative deviations of the hemodynamic parameters in the area of enhancement compared with the rest of the venous vascular surface indicate a mean reduction of AWSS (-44.5 %) and OSI (-13.0 %) whereas RRT (+40.0 %) shows an increase. These local quantitative investigations confirm the initial qualitative observations and are visualized in the boxplots (see Figure 6).

4. DISCUSSION

The hemodynamics of draining veins of cerebral AVMs are presently not well understood. In particular, local enhancements in the vessel walls of these veins, which are detected in the VW-MRI data, have not been analyzed with respect to underlying hemodynamics. This interdiciplinary approach investigates time-dependent hemodynamic information at local signal enhancements in vessel walls of draining veins to improve the understanding of cerebral AVMs. Patient-specific 3D models of venous vascular anatomy could be generated based on multimodal imaging data for eight patients whose AVMs showed different complexities with respect to their courses and number of draining veins.

The time-dependent blood flow simulations based on the segmented 3D models provide the basis for the qualitative and quantitative haemodynamic observations of the draining veins. By obtaining patient-specific flow quantification measurements using 2D PC MRI on the draining veins and the main veins, it is possible to define patient-specific boundary conditions at almost all inlets and outlets for each model. The combination of patient-specific vascular models with a high number of venous vessels with the corresponding *in vivo* measured flow data enable the performance of realistic simulations.

To investigate the impact of hemodynamics along the vessel wall, especially locally in the area of a present signal enhancement, the three shear-related parameters AWSS, OSI and RRT are chosen. These parameters are considered to be of special relevance in neurovascular research and can provide information about possible pathological changes [14, 15, 16]. Accordingly, these parameters can provide information about vascular alteration processes, allowing conclusions to be drawn about the states of vessel walls. In blood vessels, WSS acts mainly on the endothelium, the innermost layer of the vessel wall, and is considered a critical parameter affecting vascular changes [17]. While numerous hemodynamic studies for cerebral aneurysms show the influence of WSS on rupture risk [18], the effects of WSS in AVMs are poorly understood. Some studies analyzed WSS in the feeding arteries of AVMs. These reveal increased WSS in the feeding arteries compared with the contralateral ones [16], with this effect being particularly evident in symptomatic AVMs [19]. However, no such observations have been made for draining veins, so that it is not possible to compare these results with the findings of this work. The OSI and RRT are also considered critical parameters for rupture risk analysis of cerebral aneurysms [20, 21]. Specifically,

WSS, OSI and RRT could already be investigated for signal-enhanced aneurysms. In particular, low shear stress and increased OSI and RRT values have already been correlated with signal amplifications in the vessel walls of cerebral aneurysms [22, 23, 24].
The qualitative results of the hemodynamic simulations show the local expressions of these shear-related parameters in the area of the identified signal amplifications. For most patients, especially low AWSS and high RRT values are found in the enhanced areas. In contrast, no clear tendencies can be identified for the OSI on the basis of the qualitative analyses. Since the qualitative representations only provide a visual impression of the distributions of the hemodynamic parameters on the vessel wall, the tendencies were examined more precisely on the basis of quantitative investigations. The global comparison of the 15 draining veins also shows that enhanced draining veins have overall lower AWSS and OSI and higher RRT values. These results confirm previous studies in which signal enhancement was found in the vessel wall, especially in aneurysms with low global AWSS [22]. However, it is critical to associate global hemodynamic investigations with highly localized signal enhancement. The areas of enhancement cover only a very small part of the vascular surface in draining veins. For this reason, the quantitative analysis is also performed in the locally limited areas of enhancement. The relative parameter deviations within these areas show a clear tendency, especially for the AWSS and confirm the initial qualitative observations of the local behavior. With the lowest variation around the mean value, this parameter is characterized as the most stable in its behavior in the signal enhancement. For the RRT, the observed qualitative characteristics are also confirmed by the relative deviations. Here, the distribution around the average value is higher compared to the AWSS. For the OSI, the quantitative observations must be critically evaluated. Due to the very small range of values in both the enhanced and the non-enhanced regions, there are high variations in the relative deviations. Therefore, the behavior of the OSI cannot be associated with the occurrence of vessel wall enhancement. For the AWSS, on the other hand, a relationship from locally low shear stress to the occurrence of enhancement can be established. These have been increasingly associated with inflammatory processes in the vessel wall using VW-MRI [25, 26] and low shear stress can be associated with vessel wall inflammation [27]. Accordingly, this supports the findings of the study. Due to the indirect proportionality of the RRT to the AWSS [28], it is possible to attribute the locally increased RRT values to the occurrence of local signal amplifications as well.
The key findings of this study confirm existing observations regarding the behaviour of AWSS and RRT for enhanced vascular structures. By applying these findings to venous areas of AVMs that have been poorly studied so far, new possibilities arise in the risk assessment of this disease. Inflammatory processes in the vessel walls, which often cause further pathological diseases, can be attributed to low tangential forces and high residence times of the blood on the vessel wall.

Limitations: The presented approach has several limitations. First, numerous manual image processing steps are necessary to generate the patient-specific 3D models. In particular, the local smoothing operations can artificially alter the model and cause it to deviate from the patient-specific morphology. To avoid this, continuous comparison with various angiographic data is necessary, which is time-consuming.
Furthermore, the enhanced areas projected onto the venous models are not fully representing the real wall enhancement. Due to the manual registration method, there may be slight deviations in the exact position. Due to the contour-based segmentation method, the enhanced structures are extracted as areas of constant intensity. This makes it impossible to show different intensity levels of signal amplification on the vessel wall of the draining veins. For this reason, the areas on the vein could only be divided into enhanced and non-enhanced areas, thus the calculated hemodynamic parameters could only be correlated with the occurrence of an enhancement and not with an intensity level. Within the hemodynamic simulations, several simplifications are made, such as the use of constant pressure values at unknown vessel cross-sections or the assumption of rigid walls. In particular, model simplification to rigid wall conditions is a well-known problem in numerical flow simulation for neurovascular vessels. Especially, for the consideration of shear-related parameters on the vessel wall, an integration of information such as patient-specific wall properties would be beneficial. However, the modelling of vessel wall boundary conditions is only advantageous if corresponding reliable wall information from the respective patient exists. Since such information could not be obtained from the available image data, no modelling of vessel wall boundary conditions was performed in this work. Simplified assumptions such as constant wall thicknesses, on the other hand, can lead to erroneous results [29].
Finally, the lack of consideration of the nidus for the hemodynamic considerations must be mentioned. Existing studies already modelled realistic nidus vessels for the validation of CFD simulations [30]. For the investigations of this work, however, the exclusion of the nidus can be considered acceptable. Measured patient-specific flow rates were defined at the inlets of the draining veins and thus the hemodynamic influence of the nidus was included. In addition, this reduced the calculation times for the numerical simulations.
Despite these limitations, this study provides initial insights into the hemodynamic characteristics of AVM draining veins. The developed approach,

which is performed for eight patients, forms a basis for the investigation of further patients with signal-enhanced veins of AVMs. This can strengthen hemodynamic understanding and thus provide further insight into the relationship between promising biomarkers in imaging data and the underlying physical cause.

5. CONCLUSION

The study addresses the hemodynamic investigation of draining veins of cerebral AVMs with local wall enhancement detectable in the VW-MRI data. The developed approach allows to process multimodal medical image data. Previously verified local vessel wall signal enhancements are manually extracted and mapped onto the surface of these models after appropriate co-registration with the luminal vessel models. Based on the venous vessel models, time-dependent numerical blood flow simulations are carried out. Due to the availability of patient-specific blood flow quantifications, these could be defined as in- and outlet boundary conditions for the haemodynamic simulations, thus ensuring reliable blood flow prediction. By visualizing the simulation results with overlaid wall enhancement, qualitative trends in hemodynamic behavior could be observed within the enhanced regions. These tendencies could also be demonstrated with the help of a quantitative analysis. Thus, it is possible to consider potential correlations between signal-enhanced vascular regions and local decreases (AWSS, OSI) or increases (RRT) of hemodynamic parameter values.

ACKNOWLEDGEMENTS

This work is partly funded by the Federal Ministry of Education and Research within the Forschungscampus *STIMULATE* (grant no. 13GW0473A) and the German Research Foundation (BE 6230/6-1). The authors state no conflict of interest.

REFERENCES

[1] Choi, J. H., Mast, H., Sciacca, R. R., Hartmann, A., Khaw, A. V., Mohr, J. P., Sacco, R. L., and Stapf, C., 2006, "Clinical Outcome After First and Recurrent Hemorrhage in Patients With Untreated Brain Arteriovenous Malformation", *Stroke*, Vol. 37 (5), pp. 1243–1247.

[2] Lin, T. M., Yang, H. C., Lee, C. C., Wu, H. M., Hu, Y. S., Luo, C. B., Guo, W. Y., Kao, Y. H., Chung, W. Y., and Lin, C. J., 2020, "Stasis Index from Hemodynamic Analysis using Quantitative DSA correlates with Hemorrhage of Supratentorial Arteriovenous Malformation: A Cross-sectional Study", *Journal of Neurosurgery*, Vol. 132 (5), pp. 1574–1582.

[3] Mohr, J. P., Kejda-Scharler, J., and Pile-Spellman, J., 2013, "Diagnosis and Treatment of Arteriovenous Malformations", *Current Neurology and Neuroscience Reports*, Vol. 13 (2).

[4] Takeda, Y., Kin, T., Sekine, T., Hasegawa, H., Suzuki, Y., Uchikawa, H., Koike, T., Kiyofuji, S., Shinya, Y., Kawashima, M., and Saito, N., 2021, "Hemodynamic Analysis of Cerebral AVMs with 3D Phase-Contrast MR Imaging", *American Journal of Neuroradiology*, Vol. 42 (12), pp. 2138–2145.

[5] Frey, S., Cantieni, T., Vuillemin, N., Haine, A., Kammer, R., von Tengg-Kobligk, H., Obrist, D., and Baumgartner, I., 2018, "Angioarchitecture and Hemodynamics of Microvascular Arterio-Venous Malformations", *PLOS ONE*, Vol. 13 (9), p. e0203368.

[6] Chenoune, Y., Tankyevych, O., Li, F., Piotin, M., Blanc, R., and Petit, E., 2019, "Three-dimensional Segmentation and Symbolic Representation of Cerebral Vessels on 3DRA Images of Arteriovenous Malformations", *Computers in Biology and Medicine*, Vol. 115, p. 103489.

[7] Ho, H., Mithraratne, K., and Hunter, P., 2013, "Numerical Simulation of Blood Flow in an Anatomically-Accurate Cerebral Venous Tree", *IEEE Transactions on Medical Imaging*, Vol. 32 (1), pp. 85–91.

[8] Miraucourt, O., Salmon, S., Szopos, M., and Thiriet, M., 2016, "Blood Flow in the Cerebral Venous System: Modeling and Simulation", *Computer Methods in Biomechanics and Biomedical Engineering*, Vol. 20 (5), pp. 471–482.

[9] Edjlali, M., Guédon, A., Hassen, W. B., Boulouis, G., Benzakoun, J., Rodriguez-Régent, C., Trystram, D., Nataf, F., Meder, J.-F., Turski, P., Oppenheim, C., and Naggara, O., 2018, "Circumferential Thick Enhancement at Vessel Wall MRI Has High Specificity for Intracranial Aneurysm Instability", *Radiology*, Vol. 289 (1), pp. 181–187.

[10] Larsen, N., Flüh, C., Saalfeld, S., Voß, S., Hille, G., Trick, D., Wodarg, F., Synowitz, M., Jansen, O., and Berg, P., 2020, "Multimodal Validation of Focal Enhancement in Intracranial Aneurysms as a Surrogate Marker for Aneurysm Instability", *Neuroradiology*, Vol. 62 (12), pp. 1627–1635.

[11] Küker, W., Gaertner, S., Nagele, T., Dopfer, C., Schoning, M., Fiehler, J., Rothwell, P. M., and Herrlinger, U., 2008, "Vessel Wall Contrast Enhancement: A Diagnostic Sign of Cerebral Vasculitis", *Cerebrovascular Diseases*, Vol. 26 (1), pp. 23–29.

[12] Alaraj, A., Amin-Hanjani, S., Shakur, S. F., Aletich, V. A., Ivanov, A., Carlson, A. P., Oh, G., and Charbel, F. T., 2015, "Quantitative Assessment of Changes in Cerebral Arteriovenous Malformation Hemodynamics After Embolization", *Stroke*, Vol. 46 (4), pp. 942–947.

[13] Guglielmi, G., 2008, "Analysis of the Hemodynamic Characteristics of Brain Arteriovenous Malformations using Electrical Models", *Neurosurgery*, Vol. 63 (1), pp. 1–11.

[14] Cebral, J., Mut, F., Weir, J., and Putman, C., 2010, "Association of Hemodynamic Characteristics and Cerebral Aneurysm Rupture", *American Journal of Neuroradiology*, Vol. 32 (2), pp. 264–270.

[15] Xiang, J., Tutino, V., Snyder, K., and Meng, H., 2013, "CFD: Computational Fluid Dynamics or Confounding Factor Dissemination? The Role of Hemodynamics in Intracranial Aneurysm Rupture Risk Assessment", *American Journal of Neuroradiology*, Vol. 35 (10), pp. 1849–1857.

[16] Alaraj, A., Shakur, S. F., Amin-Hanjani, S., Mostafa, H., Khan, S., Aletich, V. A., and Charbel, F. T., 2015, "Changes in Wall Shear Stress of Cerebral Arteriovenous Malformation Feeder Arteries After Embolization and Surgery", *Stroke*, Vol. 46 (5), pp. 1216–1220.

[17] Epstein, F. H., Gibbons, G. H., and Dzau, V. J., 1994, "The Emerging Concept of Vascular Remodeling", *New England Journal of Medicine*, Vol. 330 (20), pp. 1431–1438.

[18] Meng, H., Tutino, V., Xiang, J., and Siddiqui, A., 2013, "High WSS or Low WSS? Complex Interactions of Hemodynamics with Intracranial Aneurysm Initiation, Growth, and Rupture: Toward a Unifying Hypothesis", *American Journal of Neuroradiology*, Vol. 35 (7), pp. 1254–1262.

[19] Chang, W., Loecher, M., Wu, Y., Niemann, D., Ciske, B., Aagaard-Kienitz, B., Kecskemeti, S., Johnson, K., Wieben, O., Mistretta, C., and Turski, P., 2012, "Hemodynamic Changes in Patients with Arteriovenous Malformations Assessed Using High-Resolution 3D Radial Phase-Contrast MR Angiography", *American Journal of Neuroradiology*, Vol. 33 (8), pp. 1565–1572.

[20] Berg, P., and Beuing, O., 2017, "Multiple Intracranial Aneurysms: A Direct Hemodynamic Comparison between Ruptured and Unruptured Vessel Malformations", *International Journal of Computer Assisted Radiology and Surgery*, Vol. 13 (1), pp. 83–93.

[21] Neyazi, B., Swiatek, V. M., Skalej, M., Beuing, O., Stein, K.-P., Hattingen, J., Preim, B., Berg, P., Saalfeld, S., and Sandalcioglu, I. E., 2020, "Rupture Risk Assessment for Multiple Intracranial Aneurysms: Why there is no Need for Dozens of Clinical, Morphological and Hemodynamic Parameters", *Therapeutic Advances in Neurological Disorders*, Vol. 13, p. 175628642096615.

[22] Zhang, M., Peng, F., Tong, X., Feng, X., Li, Y., Chen, H., Niu, H., Zhang, B., Song, G., Li, Y., Liu, P., Liu, A., and Li, R., 2021, "Associations between Haemodynamics and Wall Enhancement of Intracranial Aneurysm", *Stroke and Vascular Neurology*, Vol. 6 (3), pp. 467–475.

[23] Veeturi, S. S., Rajabzadeh-Oghaz, H., Pintér, N. K., Waqas, M., Hasan, D. M., Snyder, K. V., Siddiqui, A. H., and Tutino, V. M., 2021, "Aneurysm Risk Metrics and Hemodynamics are Associated with Greater Vessel Wall Enhancement in Intracranial Aneurysms", *Royal Society Open Science*, Vol. 8 (11).

[24] Lv, N., Karmonik, C., Chen, S., Wang, X., Fang, Y., Huang, Q., and Liu, J., 2020, "Wall Enhancement, Hemodynamics, and Morphology in Unruptured Intracranial Aneurysms with High Rupture Risk", *Translational Stroke Research*, Vol. 11 (5), pp. 882–889.

[25] Young, C. C., Bonow, R. H., Barros, G., Mossa-Basha, M., Kim, L. J., and Levitt, M. R., 2019, "Magnetic Resonance Vessel Wall Imaging in Cerebrovascular Diseases", *Neurosurgical Focus*, Vol. 47 (6), p. E4.

[26] Lehman, V. T., Brinjikji, W., Mossa-Basha, M., Lanzino, G., Rabinstein, A. A., Kallmes, D. F., and Huston, J., 2018, "Conventional and High-resolution Vessel Wall MRI of Intracranial Aneurysms: Current Concepts and New Horizons", *Journal of Neurosurgery*, Vol. 128 (4), pp. 969–981.

[27] Traub, O., and Berk, B. C., 1998, "Laminar Shear Stress: Mechanisms by which Endothelial Cells Transduce an Atheroprotective Force", *Arteriosclerosis, Thrombosis, and Vascular Biology*, Vol. 18 (5), pp. 677–685.

[28] Himburg, H. A., Grzybowski, D. M., Hazel, A. L., LaMack, J. A., Li, X.-M., and Friedman, M. H., 2004, "Spatial Comparison between Wall Shear Stress Measures and Porcine Arterial Endothelial Permeability", *American Journal of Physiology-Heart and Circulatory Physiology*, Vol. 286 (5), pp. H1916–H1922.

[29] Voß, S., Glaßer, S., Hoffmann, T., Beuing, O., Weigand, S., Jachau, K., Preim, B., Thévenin, D., Janiga, G., and Berg, P., 2016, "Fluid-Structure Simulations of a Ruptured Intracranial Aneurysm: Constant versus Patient-Specific Wall Thickness", *Computational and Mathematical Methods in Medicine*, Vol. 2016, pp. 1–8.

[30] Kaneko, N., Ullman, H., Ali, F., Berg, P., Ooi, Y. C., Tateshima, S., Colby, G. P., Komuro, Y., Hu, P., Khatibi, K., Mejia, L. L. P., Szeder, V., Nour, M., Guo, L., Chien, A., Vinuela, F., Nemoto, S., Mashiko, T., Sehara, Y., Hinman, J. D., Duckwiler, G., and Jahan, R., 2020, "In Vitro Modeling of Human Brain Arteriovenous Malformation for Endovascular Simulation and Flow Analysis", *World Neurosurgery*, Vol. 141, pp. e873–e879.